ponent **5** exhibits significant inhibitory activity at dosages of 60 to 250 μg per kilogram of body weight against the P-388 leukemia in mice (*3*).

The tumor inhibitory principles of *Croton* oil were divided into two active fractions on solvent partition between 10 percent aqueous methanol and Skellysolve B. Column chromatography of the residue from the aqueous methanol solution over SilicAR CC-7 deactivated by water and subsequent TLC and high-pressure liquid chromatography were guided in a manner analogous to that described for *E. esula*. This procedure led to the isolation of an active principle as a resinous material (*4*) (0.048 percent of the weight of *Croton* oil) with specific optical rotation at 27° for the sodium D line ($[\alpha]_D^{27}$) + 39° (*c*, 0.78, dioxane); HRMS showed the molecular ion at *m/e* 600.3550 (calculated, 600.3662). Comparison of the $[\alpha]_D$, ultraviolet, infrared, NMR, and mass spectra with those described for phorbol 12-tiglate 13-decanoate (*10*) indicated that the active constituent was **5**.

A series of commercially available (*8*) *Croton* oil principles (**6** to **9**) were assayed against P-388 lymphocytic leukemia in order to determine the potential significance of the ester side chains and of other structural features of compounds similar to phorbol. When these materials were assayed in parallel with **5**, only phorbol 12-tiglate 13-decanoate showed antileukemic activity over the dose ranges tested.

Also, in pursuing the antileukemic principles of several plants of the family Thymelaeaceae, we have isolated several diterpenoid esters that have considerable chemical similarity to the newly characterized principles of the Euphorbiaceae (*11*). In view of our earlier findings (*11, 12*), it will be of interest to determine the significance of various structural features for the antileukemic activity of the diterpenoid esters. Such studies may clarify also the paradoxical similarity in structure between the cocarcinogenic and antileukemic principles of the Euphorbiaceae and the Thymelaeaceae.

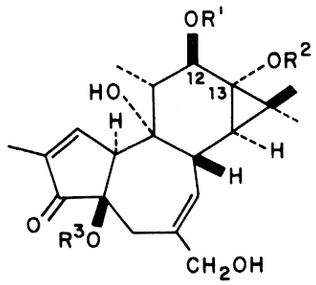

5 R^1 = CO - $(CH_3)C = CHCH_3$; R^2 = CO - $(CH_2)_8$ - CH_3; R^3 = H

6 $R^1 = R^2 = R^3$ = H

7 R^1 = CO - $(CH_2)_{12}$ - CH_3; R^2 = $COCH_3$; R^3 = H

8 R^1 = CO - $(CH_2)_{12}$ - CH_3; R^2 = $COCH_3$; R^3 = CH_3

9 $R^1 = R^2$ = COC_6H_5, R^3 = H

S. MORRIS KUPCHAN
I. UCHIDA, A. R. BRANFMAN
R. G. DAILEY, JR., B. YU FEI
Department of Chemistry,
University of Virginia, Charlottesville 2290

References and Notes

1. J. L. Hartwell, *Lloydia* **32**, 153 (1969).
2. *Euphorbia esula* L. (whole plant) was collected in Marinette County, Wisconsin, in July 1966. We thank H. H. Iltis of the University of Wisconsin for confirming the identity of the plant. A voucher specimen is deposited in the University of Wisconsin Herbarium.
3. Tumor-inhibitory activity was assayed under the auspices of the National Cancer Institute as described by R. I. Geran, N. H. Greenberg, M. M. McDonald, A. M. Schumacher, and B. J. Abbott [*Cancer Chemother. Rep. Part 3* **3**, 1 (1972)]. Evaluation of antileukemic assay results on a statistical basis in sequential testing is such that a material is considered active if it causes an increase in survival of treated animals (T) over controls (C) resulting in T/C ≥ 125 percent.
4. The homogeneity of the material was confirmed by TLC with several solvent systems and by high-pressure liquid chromatography.
5. Additional physical constants for **1** are: ultraviolet absorption maximum (ethanol) (log ε), 230 (4.46), 272 (3.37), 280 (3.31) nm; infrared absorption maximum (chloroform), 2.86, 3.45, 3.52, 5.82, 5.85, 7.88 μm; nuclear magnetic resonance spectrum (deuterochloroform) τ 8.96 (3H, d, H_3-18), 8.93 (6H, s, H_3-16,-17), 8.16 (3H, br s, H_3-19), 6.02 (1H, s, H-5), 5.84 (1H, dd, *J* = 11, 4 hertz, H-8), 5.09 (2H, AB q, H_2-20), 4.22 (1H, s, H-3), 3.87 (1H, br s, H-1), 3.76 (1H, d, *J* = 4 hertz, H-7), 2.5 (6H, m, two of B_2X portion of A_2B_2X, *m*- and *p*-benzoate protons), 1.96 (4H, two of A_2 portion of A_2B_2X, *o*-benzoate protons); mass spectrum *m/e* 556 (M^+), 538, 434, 416, 312, 294.
6. K. Zechmeister, F. Brandl, W. Hoppe, E. Hecker, H. J. Opferkuch, W. Adolf, *Tetrahedron Lett.* (1970), p. 4075.
7. In (*6*), the signals at τ 5.68 and 6.21 in the NMR spectrum of ingenol were assigned as either H-3 or H-5. Spin decoupling [T. H. Siddall and W. E. Stewart, *Prog. Nucl. Magn. Reson. Spectrosc.* **5**, 33 (1969); L. M. Jackman and S. Sternhell, *Applications of Nuclear Magnetic Resonance Spectroscopy in Organic Chemistry* (Pergamon, New York, ed. 2, 1969), p. 368] and internuclear double resonance [W. von Phillipsborn, *Angew. Chem. Int. Ed. Engl.* **10**, 472 (1971)] experiments in this laboratory allowed assignment of the former signal as H-3 and the latter as H-5.
8. *Croton* oil and the irritant and cocarcinogenic active principles of the oil were purchased from Consolidated Midland Corporation, Chemical Division, Brewster, New York.
9. E. Hecker and R. Schmidt, *Prog. Chem. Org. Nat. Prod.* **31**, 377 (1974).
10. E. Hecker and E. Clarke, *Z. Krebsforsch.* **67**, 192 (1965).
11. S. M. Kupchan, J. G. Sweeny, R. L. Baxter, T. Murae, V. A. Zimmerly, B. R. Sickles, *J. Am. Chem. Soc.* **97**, 672 (1975); S. M. Kupchan and R. L. Baxter, *Science* **187**, 652 (1975).
12. S. M. Kupchan, *Fed. Proc. Fed. Am. Soc. Exp. Biol.* **33**, 2288 (1974); *Recent Adv. Phytochem.* **9**, 167 (1975).
13. This report is part 112 in the series entitled "Tumor Inhibitors"; part 111 is by S. M. Kupchan, C. W. Sigel, M. J. Matz, C. J. Gilmore, and R. F. Bryan [*J. Am. Chem. Soc.*, in press]. Supported by grant CA-11718 and contract NO1-CM-12099 from the National Cancer Institute and grant CI-102J from the American Cancer Society. A.R.B. was an NIH postdoctoral fellow, 1972 through 1975. We thank B. R. Sickles for technical assistance.

20 October 1975

Representation of the Visual Field on the Medial Wall of Occipital-Parietal Cortex in the Owl Monkey

Abstract. *The medial visual area is located on the medial wall of occipital-parietal cortex. A much larger proportion of this area is devoted to the representation of the more peripheral parts of the visual field than in any other cortical area or subcortical visual structure that has been mapped previously in any species of primate.*

In the representations of the visual field in almost all of the cortical visual areas and in the subcortical visual structures in primates, a very large proportion of each visuotopic map is devoted to the representation of the small central part of the visual field in which primates see with high acuity (*1*). Described in this report is the single known exception to this rule, the medial visual area, which is located on the medial wall of occipital-parietal cortex. A much greater proportion of the medial area is devoted to the representation of the relatively more peripheral parts of the visual field than in any other visuotopically organized cortical area or in any subcortical visual structure, including the lateral geniculate nucleus, inferior pulvinar, or superior colliculus, that has been mapped in any primate. Each of these representations of the visual field is likely to perform its own set of functions in the analysis and integration of visual information, and in whatever functions that are performed by the medial area there appears to be a considerably greater emphasis on input from the more peripheral parts of the visual field.

This study is part of a series of investigations in which we have sought to identify and determine the organization of the major functional units, the neural representations of the visual field, in the visual system of primates. In most of these investigations, we have explored the cerebral cortex because this structure contains the great bulk of the neurons involved in the processing of visual information. The owl monkey (*Aotus trivirgatus*) was chosen as our experimental animal because the cerebral cortex is relatively less convoluted in this species than in most other simian primates, thus facilitating our task of mapping the representations of the visual field in the cortex. In this part of the total

project, the visuotopic organization of the medial occipital-parietal cortex was explored with electrophysiological mapping techniques in five owl monkeys (*2*). The monkeys were anesthetized with urethan and prepared for recording. Tungsten and platinum-iridium microelectrodes were used to record from small clusters of neurons or occasionally from single neurons in tangential penetrations parallel to the medial surface of occipital-parietal cortex. Receptive fields were plotted by moving circular spots or rectangular slits and bars on the surface of a translucent plastic hemisphere centered in front of the contralateral eye. The position of the optic disk was projected onto the plastic hemisphere with the method of Fernald and Chase (*3*). The ipsilateral eye usually was covered with an opaque shield. Electrode tracks and recording sites were reconstructed from histological sections and photographs of the intact brain.

Figure 1 illustrates the data from our most complete mapping of the medial area; data obtained in the other four experiments revealed the same pattern of visuotopic organization. Tangential penetrations 1 through 4 ran parallel to the medial surface of occipital-parietal cortex at a distance of approximately 1 mm from the medial surface. In previously published experiments, we found that the receptive fields recorded adjacent to the medial area in the second visual area (V II) were located in the lower quadrant near the horizontal meridian about 50° to 60° from the center (*4*). Thus, as is shown in Fig. 1, and also in Fig. 2, which illustrates the organization of the other cortical visual areas that have been mapped in the owl monkey, the border between the medial area and the second visual area corresponds to a peripheral portion of the horizontal meridian. In other experiments in the dorsomedial area, we found that receptive fields recorded near its common border with the medial area began near the vertical meridian in the lower quadrant and proceeded in a broad loop in the periphery toward the horizontal meridian (*5*). Thus, as is shown in Figs. 1 and 2, the common border between the dorsomedial and the medial areas corresponds to part of the lower field vertical meridian and the peripheral portions of the lower visual quadrant. Dorsally, the medial area is adjoined by poste-

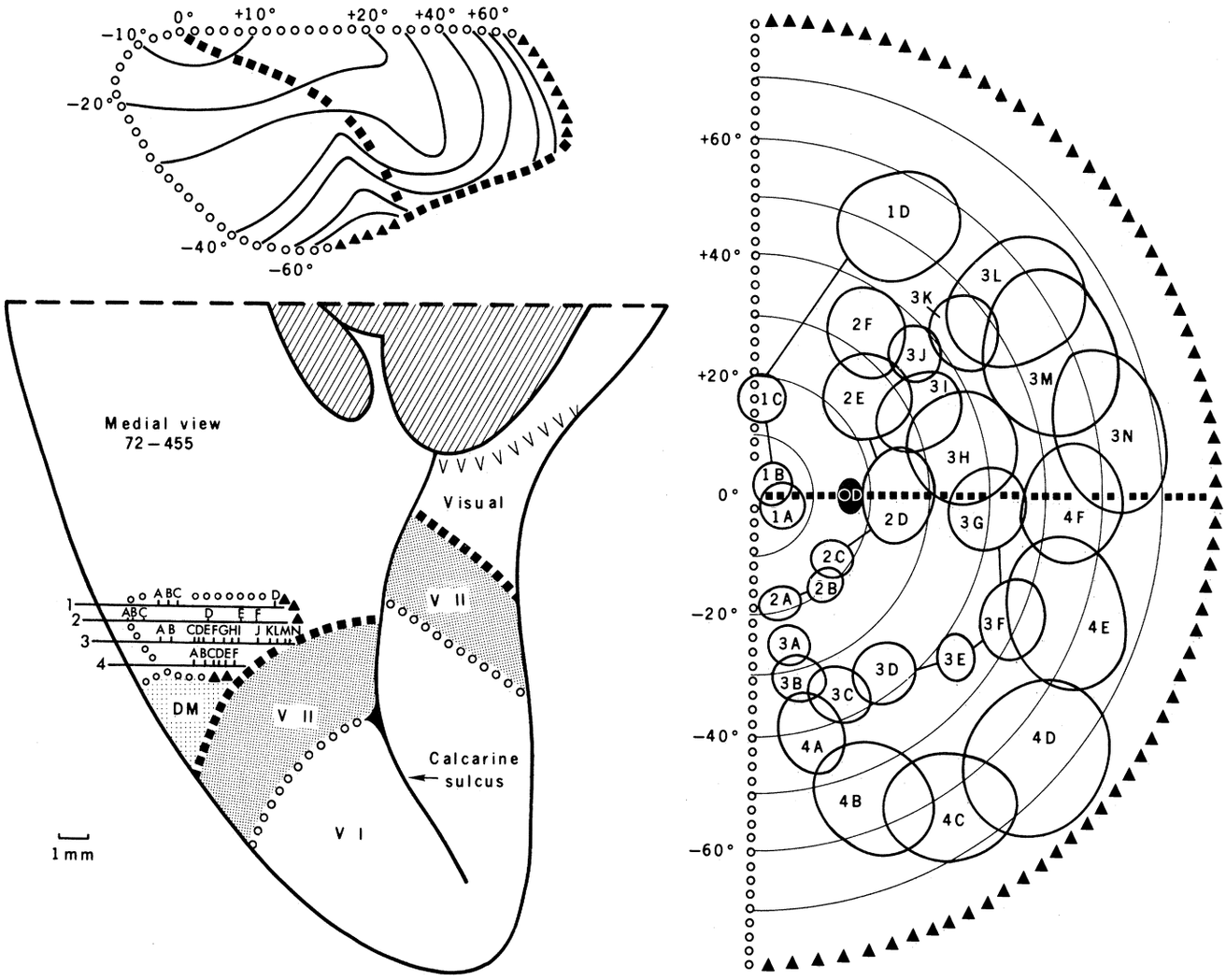

Fig. 1. Microelectrode recording penetrations and receptive field data for the medial visual area in owl monkey 72-455. The diagram on the lower left is a view of the posterior half of the medial wall of cerebral cortex of the left hemisphere with the brainstem and cerebellum removed. Anterior is up and dorsal is to the left in this diagram. Microelectrode penetrations are numbered, and recording sites are indicated by short bars denoted by letters. The corresponding receptive fields are shown in the perimeter chart on the right. In the upper left is an expanded map of the visuotopic organization of the medial area. The circles indicate the representation of the vertical meridian (midline) of the visual field; the squares indicate the horizontal meridian of the contralateral half of the visual field; the triangles indicate the temporal periphery of the contralateral hemifield. *V I* is the first visual area; *V II* is the second visual area; *DM* is the dorsomedial visual area. *OD* indicates the projection of the optic disk or blind spot.

rior parietal cortex, where we have mapped receptive fields so large that it is not clear whether any visuotopic organization exists in this region. Posterior parietal cortex corresponds in location to area 7, which in alert macaque monkeys has been found to contain many neurons which are activated when the monkey directs his gaze toward wanted objects within his reach or when the monkey visually tracks such objects (*6*). Anteriorly, the medial area is adjoined by parietal cortex on the medial wall which did not respond to visual stimulation in our experiments.

The detailed visuotopic organization of the medial area is illustrated in the expanded map in the upper left corner of Fig. 1. The medial area is not a simple topological or first-order transformation of the contralateral half of the visual field; instead, as in the second visual area, the dorsomedial area, and the dorsolateral crescent, the medial area is a second-order transformation in which adjacent points in the contralateral half of the visual field are *not* always represented in adjacent points in the cortical map (*7*). In the medial area, points *just above* the representation of the horizontal meridian more than 50° from the center are adjacent to points in the second visual area rather than points *just below* the horizontal meridian in the medial area. However, while the medial area may be classified as a second-order transformation of the contralateral hemifield, the disruption of the topological relationship between different parts of the hemifield is much less extensive in the medial area than in the second visual area, the dorsomedial area, or the dorsolateral crescent.

Although the response properties of neurons in the medial area were not studied in detail, we did notice that the neurons usually responded as well to circular spots as to rectangular stimuli and that the orientation of the rectangular stimuli was not critical.

Approximately 96 percent of the medial visual area is devoted to the representation of the parts of the visual field more than 10° from the center, and possibly correlated with this are the results of a recent autoradiographic study of the projections of the first visual area in the squirrel monkey by Martinez-Millan and Hollander (*8*). These authors found that the portion of the first visual area that is located on the lateral surface of the occipital lobe, and which corresponds to the representation of the central part of the visual field, projects to two cortical loci which they termed "provisional area 18" and "cortex near the superior temporal sulcus." These results agree very closely with earlier studies done in the squirrel monkey by Spatz, Tigges, and Tigges (*9*), and it is very likely that these two cortical projections are to the second visual area and the middle temporal area. However, when Martinez-Millan and Hollander studied the projections of the portions of the first visual area that are located on the medial wall of the hemisphere and in the calcarine sulcus where the more peripheral parts of the visual field are represented, they found that in addition to the two previously mentioned loci there was a third locus in the parieto-occipital sulcus on the medial wall. This third projection, which arises only from the more peripheral parts of the first

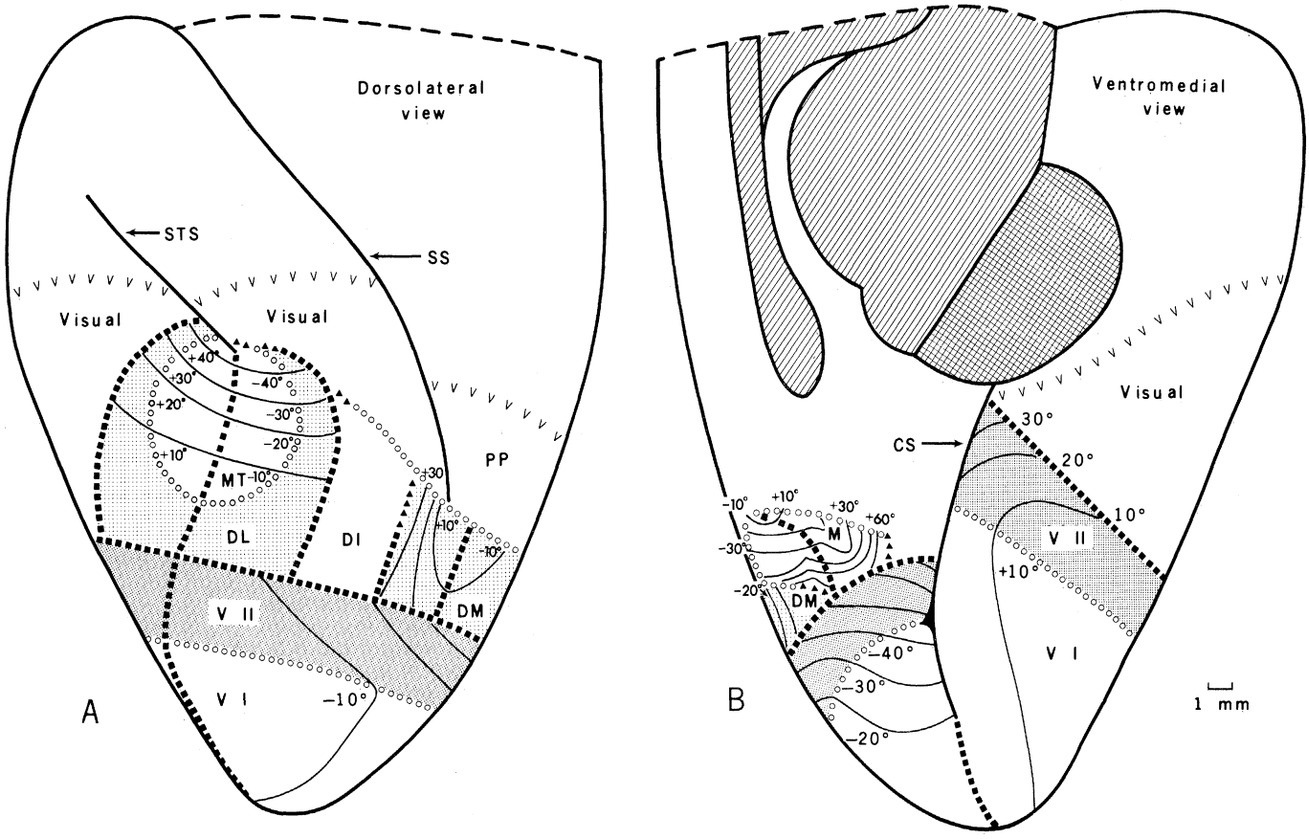

Fig. 2. Representations of the visual field in the cerebral cortex of the owl monkey. (A) A dorsolateral view of the posterior two-thirds of the left cerebral hemisphere. (B) A ventromedial view of the posterior two-thirds of the left cerebral hemisphere in which the brainstem and cerebellum have been removed to expose the ventral surface of the occipital and temporal lobes. *DL* (dorsolateral crescent), *DI* (dorsointermediate area), *DM* (dorsomedial area), and *M* (medial area) comprise the *third tier* of cortical visual areas; *V I* constitutes the first tier and *V II* the second. DI's borders have been definitely established, but DI has not yet been mapped in detail. *MT* (middle temporal area) is a fourth tier cortical visual area. Meridians are not necessarily continuous between adjacent cortical visual areas; such discontinuities occur at "incongruent borders" between areas (*5*). The rows of *V*'s indicate the anterior border of visually responsive cortex. In the cortex marked *Visual* there exist additional representations of the visual field that have not yet been mapped in detail. *PP* is posterior parietal cortex; *STS* is the superior temporal sulcus; *SS* is the sylvian sulcus; and *CS* is the calcarine sulcus. Other conventions and abbreviations are the same as in Fig. 1.

visual area, corresponds very closely in location to the medial area in the owl monkey. Our interpretation of Martinez-Millan and Hollander's results is that there may exist a projection from the peripheral parts of the first visual area to the medial area and that this projection may be related to the relatively large representation of the more peripheral portions of the visual field in the medial area (*10*). In addition, there exist other probable projections to the medial area from the middle temporal area and the dorsomedial area. Spatz and Tigges (*11*) found in marmosets that the middle temporal area projects to a zone on the medial wall of occipital-parietal cortex (their focus 6), which corresponds very closely in location to the medial area, and Wagor *et al.* (*11*) found in the owl monkey that the dorsomedial area projects to the medial area.

Adjoining the anterior border of the second visual area are four visual areas: the dorsolateral crescent, the dorsointermediate area, the dorsomedial area, and the medial area. Collectively these areas comprise a *third tier* of cortical visual areas with the primary visual area (V I) constituting the first tier and V II the second tier. In the third tier, the relative proportion of each area devoted to the central versus the more peripheral portions of the visual field differs greatly from area to area. In the dorsolateral crescent, approximately 75 percent of the area is devoted to the portion of the visual field within 10° of the center, while only about 4 percent of the medial area is devoted to the same portion of the visual field within 10° of the center. These differences in visuotopic organization in the *third tier* suggest that in the dorsolateral crescent, which emphasizes central vision, functions in which central vision is important, such as form perception, may predominate, while in the medial area, where the more peripheral parts of the visual field are much better represented, functions in which peripheral vision is important, such as motion perception or orientation in space, may predominate.

JOHN M. ALLMAN
Division of Biology, California Institute of Technology, Pasadena 91125

JON H. KAAS
Department of Psychology, Vanderbilt University, Nashville, Tennessee 37240

References and Notes

1. J. M. Allman and J. H. Kaas, *Brain Res.* **31**, 85 (1971); *ibid.* **35**, 89 (1971); *ibid.* **76**, 247 (1974); *ibid.* **81**, 199 (1974); *ibid.*, in press; ———, R. H. Lane, *ibid.* **57**, 197 (1973); ———, F. M. Miezin, *ibid.* **40**, 291 (1972); D. B. Bender, *Assoc. Res. Vision Ophthalmol. Abstr.* (1975), p. 16; A. Cowey, *J. Neurophysiol.* **27**, 366 (1964); M. Cynader and N. Berman, *ibid.* **35**, 187 (1972); P. M. Daniel and D. Whitteridge, *J. Physiol.* **159**, 203 (1961); G. Holmes, *Br. J. Ophthalmol.* **2**, 353 (1918); J. H. Kaas, R. W. Guillery, J. M. Allman, *Brain Behav. Evol.* **6**, 253 (1972); S. Kadoya, L. R. Wolin, L. C. Massopust, *J. Comp. Neurol.* **142**, 495 (1972); R. H. Lane, J. M. Allman, J. H. Kaas, *Brain Res.* **60**, 335 (1973); J. G. Malpeli and F. H. Baker, *J. Comp. Neurol.* **161**, 569 (1975); S. Polyak, *The Vertebrate Visual System* (Univ. of Chicago Press, Chicago, 1957); S. A. Talbot and W. H. Marshall, *Am. J. Ophthalmol.* **24**, 1255 (1941).
2. The electrophysiological mapping techniques used in this study are described in greater detail in J. M. Allman and J. H. Kaas, *Brain Res.* **35**, 89 (1971).
3. R. Fernald and R. Chase, *Vision Res.* **11**, 95 (1971).
4. See figures 2 and 4 in J. M. Allman and J. H. Kaas, *Brain Res.* **76**, 247 (1974).
5. J. M. Allman and J. H. Kaas, *ibid.* **100**, 473 (1975).
6. J. Hyvarienen and A. Poranen, *Brain* **97**, 673 (1974); V. B. Mountcastle, J. C. Lynch, A. Georgopoulos, H. Sakata, C. Acuna, *J. Neurophysiol.* **38**, 871 (1975).
7. J. M. Allman and J. H. Kaas, *Brain Res.* **76**, 247 (1974).
8. L. Martinez-Millan and H. Hollander, *ibid.* **83**, 405 (1975).
9. W. B. Spatz and J. Tigges, *ibid.* **43**, (1972); ———, M. Tigges, *J. Comp. Neurol.* **140**, 155 (1970).
10. It is unlikely that these projections from the first visual area were to the peripheral parts of a single representation corresponding to area 19 with a visuotopic organization the mirror image of area 18 (second visual area). Martinez-Millan and Hollander (*8*) found that an injection in the first visual area deep in the calcarine sulcus resulted in a projection focus in area 18 on the *lower* bank of the calcarine sulcus, but the additional projection focus, which resulted only from peripheral first visual area injections, was on the medial wall *above* the *upper* bank of the calcarine sulcus. If area 19 were organized as the mirror image of area 18, such as it is in the cat [D. H. Hubel and T. N. Wiesel, *J. Neurophysiol.* **28**, 229 (1965); R. Tusa, *Anat. Rec.* **181**, 497 (1975)], then it would be expected that both projection foci would be located on the *lower* bank of the calcarine sulcus [see Martinez-Millan and Hollander's figures 6 and 19 in (*8*)].
11. W. B. Spatz and J. Tigges, *J. Comp. Neurol.* **146**, 451 (1972); E. Wagor, C. S. Lin, J. H. Kaas, *ibid.* **163**, 227 (1975). If only the peripheral parts of the first visual area project to the medial area, then the small representation of the central visual field in the medial area must receive its input from another source, such as the dorsomedial area or the middle temporal area.
12. The experiments reported in this study were conducted at the Department of Neurophysiology, University of Wisconsin. We thank Dr. Leon Schmidt, Southern Research Institute, Birmingham, Alabama, for providing the owl monkeys. Dr. R. H. Lane and Mr. F. M. Miezin assisted in some of the data collection. Histological materials were prepared by Mrs. I. Lucey and Mrs. J. Eckleberry. Figures were drawn by Ms. D. Urban. This work was supported by NIH grants NS-05236, NS-06225, and NS-12131; NSF grant GB-36779; and an Alfred P. Sloan fellowship to J.M.A. A brief abstract of this work was published in *Anat. Rec.* **178**, 297 (1974).

16 October 1975; revised 21 November 1975

Amphibious Behavior of *Alligator mississippiensis*: Roles of a Circadian Rhythm and Light

Abstract. *Juvenile American alligators in outdoor pens moved out of and into the water at sunrise and sunset, respectively. When the natural light cycle was extended with artificial illumination, these movements gradually shifted into phase with the altered light cycles; therefore, the amphibious behavior was modulated by a circadian rhythm cued by light. Movement between land and water was characterized by a decrease in body temperature, which suggests that it was not simply a proximate heat-seeking response. After the movements had been in phase with the altered light cycles for a time, they spontaneously shifted back into phase with the natural light cycle. A changing response to light is viewed as an adaptation to seasonal changes in heat availability.*

Crocodilians utilize both aquatic and terrestrial habitats during a 24-hour cycle. Typically, they spend much of the day on land and are in the water at night. In nature, Nile crocodiles (*Crocodylus niloticus*) move with regularity out of the water at sunrise and into the water at sunset (*1, 2*). Searching for the basis of this behavior, Cloudsley-Thompson noted a daily rhythm of activity in two captive Nile crocodiles (*3*). Although he referred to this rhythm of activity as circadian, as yet no evidence has been presented to substantiate the endogenous nature of the response or to identify a periodic environmental factor that might serve as a time cue, or zeitgeber.

Here I present evidence that the amphibious behavior of juvenile alligators is regulated by an internal circadian rhythm, that light is an important zeitgeber, and that an alligator's response to light is adaptable. Although alligators are poikilothermic reptiles, their daily cycle of behavior may be governed proximally by a light-cued circadian rhythm rather than by temperature.

I studied recently captured alligators (*Alligator mississippiensis*) under semi-natural conditions. Juvenile alligators were caught in Lake Okeechobee and Lake Hicpochee near Moore Haven, Florida, in July 1972 (N = 30), and October 1973 (N = 30). They weighed 0.8 to 3.8 kg, measured 68 to 114 cm in length, and were probably 2 to 4 years old (*4*). The alligators were marked individually and maintained in two identical outdoor pens (*5*) at the Archbold Biological Station, Lake Placid, Florida (50 km northwest of the capture site). Air and water temperatures were monitored continuously in one pen. Body temperatures (T_b) were taken at varying times of the day (*6*).

The alligators were observed in the natural light-dark (LD) cycle during July and August 1972, and under natural and experimentally altered LD cycles during October and November 1973. Hourly observations were made between 0400 and 1000 (E.S.T.) and 1700 and 2400 to determine whether individual animals were on land or in the water (*7*).

In the natural photoperiod, alligators